Editors' Suggestion

One-dimensional annihilating random walk with long-range interaction

Su-Chan Park (박수찬)
Department of Physics, The Catholic University of Korea, Bucheon 14662, Republic of Korea

(Received 17 July 2020; accepted 1 September 2020; published 9 October 2020)

We study the annihilating random walk with long-range interaction in one dimension. Each particle performs random walks on a one-dimensional ring in such a way that the probability of hopping toward the nearest particle is $W = [1 - \varepsilon(x + \mu)^{-\sigma}]/2$ (the probability of moving away from its nearest particle is $1 - W$), where x is the distance from the hopping particle to its nearest particle and ε, μ, and σ are parameters. For positive (negative) ε, a particle is effectively repulsed (attracted) by its nearest particle and each hopping is generally biased. On encounter, two particles are immediately removed from the system. We first study the survival probability and the mean spreading behaves in the long-time limit if there are only two particles in the beginning. Then we study how the density decays to zero if all sites are occupied at the outset. We find that the asymptotic behaviors are classified by seven categories: (i) $\sigma > 1$ or $\varepsilon = 0$, (ii) $\sigma = 1$ and $2\varepsilon > 1$, (iii) $\sigma = 1$ and $2\varepsilon = 1$, (iv) $\sigma = 1$ and $2\varepsilon < 1$, (v) $\sigma < 1$ and $\varepsilon > 0$, (vi) $\sigma = 0$ and $\varepsilon < 0$, and (vii) $0 < \sigma < 1$ and $\varepsilon < 0$. The asymptotic behaviors in each category are universal in the sense that μ (and sometimes ε) cannot affect the asymptotic behaviors.

DOI: 10.1103/PhysRevE.102.042112

I. INTRODUCTION

The annihilating random walk and its close relative the coalescing random walk describe processes whereby diffusing particles react on encounter. In their presumably simplest setting, particles perform random walks on a d-dimensional hypercubic lattice and they undergo pairwise annihilation ($A + A \to 0$) or coalescence ($A + A \to A$) if two particles happen to occupy a same site. Due to exact solvability and wide applicability to various fields, these processes have been studied extensively for many years [1–18].

In the generic setting, hopping of each particle is symmetric in the sense that the direction of hopping is chosen with equal probability among $2d$ nearest-neighbor sites. In this case, the upper critical dimension d_c is 2 and the asymptotic behavior of particle density is universal with $t^{-d/2}$ for $d < d_c$ and t^{-1} for $d > d_c$.

It is quite natural to ask what would happen if hopping is biased. In the framework of the field theory [8,12,19–21], it is easy to understand that global bias does not affect the asymptotic behavior, because the bias is removed by the Galilean transformation [22]. By the global bias, we mean that the direction and the strength of the bias does not depend on the position of a particle.

If bias varies with position and/or time, then the Galilean transformation cannot remove the bias. This kind of bias can be relevant in the renormalization group (RG) sense and the asymptotic behavior would change. One way of implementing such a bias is to introduce a quenched noise in such a way that the strength of the bias varies from site to site [23–29].

Recently, another form of bias that cannot be removed by the Galilean transformation was introduced [30], initially motivated from opinion dynamics [31,32]. This hopping bias is implemented in such a way that a particle prefers hopping toward its nearest particle. Unlike the quenched noise, the direction of hopping depends on which configuration the system is in and, accordingly, it can change with time.

In the original setting [30], the strength of the bias does not depend on how far a walker's nearest particle is located. Then the bias is generalized in Ref. [33] such that the strength of the bias is a decreasing power-law function of the distance from a particle to its nearest one. It was found that the asymptotic behavior of the density depends on the form of the power-law function.

In this paper, we further generalize the one-dimensional annihilating random walk in Ref. [33] by allowing that a particle is repulsed by its nearest particle. As we will see, the repulsion triggers rich phenomena. In Sec. II, we define the generalized model and introduce two initial conditions that are termed as the two-particle and fully occupied initial conditions, respectively. Section III studies the system with the two-particle initial condition, focusing on survival probability and mean spreading. Section IV studies how the density behaves in the long-time limit if the system evolves from the fully occupied initial condition. In Sec. V, we summarize the result of the paper.

II. MODEL

The model is defined on a one-dimensional lattice of size L with periodic boundary conditions. Each site of this lattice is either occupied by a particle or vacant. Multiple occupancy is not allowed. We will denote the occupation number at site i by s_i, which takes either 1 or 0. For convenience, we define

$$R_i = \min\{x | s_{i+x} = 1, 1 \leqslant x \leqslant L\},$$
$$L_i = \min\{x | s_{i-x} = 1, 1 \leqslant x \leqslant L\}, \tag{1}$$

 ©2020 American Physical Society

where $i \pm L$ should be interpreted as i (periodic boundary condition). In other words, R_i (L_i) is the distance from site i to the nearest occupied site on the right- (left-) hand side.

With transition rate 1, each particle hops to one of its nearest-neighbor sites. If a particle at site i is to hop, then it must move to either site $i+1$ or site $i-1$. Probability W_i of hopping to site $i+1$ is (the probability of hopping to site $i-1$ is naturally $1-W_i$)

$$W_i = \frac{1}{2} + \frac{\varepsilon}{2}\,\mathrm{sgn}(R_i - L_i)(m_i+\mu)^{-\sigma}, \tag{2}$$

where $m_i = \min\{R_i, L_i\}$, $\mathrm{sgn}(x)(\equiv x/|x|)$ is the sign of x with $\mathrm{sgn}(0)=0$, $\sigma \geqslant 0$, and ε, μ are constants with the restriction $0 \leqslant |\varepsilon| < (1+\mu)^{\sigma}$ to ensure $0 < W_i < 1$. A particle is in a sense repulsed (attracted) by its nearest particle when ε is positive (negative). If a particle happens to jump to a site that is already occupied, then the two particles are removed in no time (pairwise annihilation).

Since hopping of a particle is significantly influenced (especially for small σ) by its nearest particle even if they are separated by a large distance, we refer to the model as the annihilating random walk with long-range interaction (AWL). As we will see soon, the sign of ε plays a crucial role. To emphasize the effect of the sign, we will also refer to the model with positive (negative) ε as the annihilating random walk with long-range repulsion (attraction), which will be abbreviated as AWLR (AWLA).

In the following sections, we study the AWL for two initial conditions. One is the two-particle initial condition in which there are only two particles in a row at $t=0$ in an infinite system. In this case, we are interested in the survival probability $S(t)$ that two particles survive up to time t and the mean distance $R(t)$ between the two particles, conditioned that they are not annihilated up to time t. The asymptotic behaviors of $S(t)$ and $R(t)$ will be studied in Sec. III.

The other is the fully occupied initial condition in which $s_i = 1$ for all i at $t=0$. In this case, we investigate the asymptotic behavior of particle density

$$\rho(t) = \frac{1}{L}\sum_i \langle s_i \rangle, \tag{3}$$

where $\langle \cdots \rangle$ stands for average over ensemble. The asymptotic behavior of the density ρ of the AWLA was first reported in Ref. [30] for $\sigma = 0$ and later in Ref. [33] for any σ, which is

$$\rho(t) \sim \begin{cases} t^{-1/(1+\sigma)}, & \sigma < 1, \\ t^{-1/2}, & \sigma \geqslant 1. \end{cases} \tag{4}$$

Throughout the paper, we write $f(x) \sim g(x)$ if

$$0 < \left| \lim_{x\to x_0} \frac{f(x)}{g(x)} \right| < \infty, \tag{5}$$

where $x_0 = 0$ or $x_0 = \infty$, depending on the context. In Sec. IV, we will investigate the asymptotic behavior of ρ for any value of ε and we will reproduce Eq. (4) for negative ε in due course.

III. SURVIVAL PROBABILITY AND MEAN SPREADING

This section studies how the system evolves if it starts from the two-particle initial condition. Let $\widetilde{P}_i(t)$ be the probability that the distance between the two particles is i at time t. $\widetilde{P}_0(t)$ is the probability that the two particles are annihilated before t. Considering that probability of hopping to the left (right) of the left particle is the same as that of hopping to the right (left) of the right particle, we write the master equation

$$\frac{1}{2}\frac{\partial \widetilde{P}_i}{\partial t} = q_{i-1}\widetilde{P}_{i-1} + (1-q_{i+1})\widetilde{P}_{i+1} - (1-\delta_{i,0})\widetilde{P}_i, \tag{6}$$

where $\delta_{i,j}$ is the Kronecker delta symbol and

$$q_i = \frac{1}{2} + \frac{\varepsilon}{2}(i+\mu)^{-\sigma}, \tag{7}$$

with $q_0 = q_{-1} = 0$. Defining $P(i,t) = \widetilde{P}(i,2t)$, we write

$$\frac{dP_i}{dt} = q_{i-1}P_{i-1} + (1-q_{i+1})P_{i+1} - (1-\delta_{i,0})P_i, \tag{8}$$

which is equivalent to a random-walk problem with an absorbing wall at the origin, interpreting i to be a site where the walker is located. In this section, we study this random walk with the initial condition $P_i(0) = \delta_{i,1}$.

We are interested in the survival probability $S(t)$ and the mean spreading $R(t)$ conditioned on survival, defined as

$$S(t) = 1 - P_0(t), \quad R(t) = \sum_{n=1}^{\infty} \frac{nP_n(t)}{S(t)}. \tag{9}$$

We will denote the probability that the walker never visits the absorbing wall by P_s, which is obtained as

$$P_s = \lim_{t\to\infty} S(t). \tag{10}$$

The continuous-time random walk is related to the discrete-time random walk in the following way. Let $d_{i,n}$ be the probability that the walker is located at site i after nth jump in the discrete-time random walk, which satisfies

$$d_{i,n+1} = q_{i-1}d_{i-1,n} + (1-q_{i+1})d_{i+1,n} + \delta_{i,0}d_{0,n}, \tag{11}$$

with the initial condition $d_i(0) = \delta_{i,1}$. Since the number of jumps up to time t follows the Poisson distribution with mean t, $P_i(t)$ can be found by

$$P_i(t) = \sum_{n=0}^{\infty} \frac{t^n}{n!} e^{-t} d_{i,n}, \tag{12}$$

which yields

$$S(t) = \sum_{n=0}^{\infty} \frac{t^n}{n!} e^{-t}\xi_n, \quad R(t) = \frac{1}{S(t)}\sum_{n=0}^{\infty} \frac{t^n}{n!} e^{-t} r_n,$$
$$\xi_n \equiv \sum_{i=1}^{\infty} d_{i,n}, \qquad r_n \equiv \sum_{i=1}^{\infty} i d_{i,n}. \tag{13}$$

For numerical studies of $S(t)$ and $R(t)$, we either use Eq. (13) with numerical calculation of $d_{i,n}$ [especially when $S(t)$ is extremely small] or perform Monte Carlo simulations of the discrete-time random walk [especially when the observation time is large or $S(t)$ at the end of the observation is larger than 10^{-10}]. As long as we are interested in the long-time behavior, whether time is continuous or discrete is immaterial in most cases with one exception in this paper.

We begin with investigating the probability $F_i(r)$ that the walker starting from site i visits site r at least once. Notice that P_s can be obtained by

$$P_s = \lim_{r\to\infty} F_1(r). \tag{14}$$

Due to the Markov property, we have a recursion relation

$$F_i = q_i F_{i+1} + (1-q_i)F_{i-1}. \tag{15}$$

Since $F_0 = 0$, we get

$$F_{i+1} - F_i = (F_i - F_{i-1})\frac{1-q_i}{q_i} = F_1 \prod_{k=1}^{i} \frac{1-q_k}{q_k}, \tag{16}$$

which, along with $F_r = 1$ by definition, gives

$$F_n(r) = \frac{G_n}{G_r}, \quad G_n \equiv 1 + \sum_{i=1}^{n-1}\prod_{k=1}^{i} \frac{1-\varepsilon(k+\mu)^{-\sigma}}{1+\varepsilon(k+\mu)^{-\sigma}}, \tag{17}$$

where $G_0 \equiv 0$ and $G_1 \equiv 1$. For $\varepsilon = 0$, we get trivially $G_n = n$ and $F_n(r) = n/r$.

For $\sigma = 0$, one can readily get

$$G_n = \frac{1+\varepsilon}{2\varepsilon}\left[1 - \left(\frac{1-\varepsilon}{1+\varepsilon}\right)^n\right], \tag{18}$$

which gives

$$P_s = \lim_{r\to\infty} G_r^{-1} = \frac{2\varepsilon}{1+\varepsilon}\Theta(\varepsilon), \tag{19}$$

where $\Theta(\cdot)$ is the Heaviside step function. Note that G_n diverges exponentially with n for $\varepsilon < 0$, which indicates that $F_1(r)$ decreases exponentially with r.

For $\sigma = 1$, we can write G_n as

$$G_n = \frac{\Gamma(1+\mu+\varepsilon)}{\Gamma(1+\mu-\varepsilon)}\sum_{i=0}^{n-1}\frac{\Gamma(i+1+\mu-\varepsilon)}{\Gamma(i+1+\mu+\varepsilon)}, \tag{20}$$

where $\Gamma(\cdot)$ is the gamma function. For $2\varepsilon = 1$, we get

$$G_n = \sum_{i=0}^{n-1}\frac{2\mu+1}{2i+2\mu+1} \sim \frac{2\mu+1}{2}\ln n. \tag{21}$$

For $2\varepsilon \neq 1$, we use an identity

$$(a-b)\frac{\Gamma(x+b)}{\Gamma(x+a+1)} = \frac{\Gamma(x+b)}{\Gamma(x+a)} - \frac{\Gamma(x+1+b)}{\Gamma(x+1+a)}, \tag{22}$$

to obtain

$$G_n = \frac{\Gamma(1+\mu+\varepsilon)\Gamma(n+1+\mu-\varepsilon)}{(1-2\varepsilon)\Gamma(1+\mu-\varepsilon)\Gamma(n+\mu+\varepsilon)} + \frac{\mu+\varepsilon}{2\varepsilon-1}. \tag{23}$$

One can readily find

$$P_s = \lim_{r\to\infty} F_1(r) = \frac{2\varepsilon-1}{\mu+\varepsilon}\Theta(2\varepsilon-1). \tag{24}$$

Unlike the case with $\sigma = 0$, P_s can be 0 even if $\varepsilon > 0$. For $2\varepsilon < 1$, G_r for large r behaves as

$$F_1(r)^{-1} = G_r \sim r^{1-2\varepsilon}, \tag{25}$$

where we have used the Stirling's formula. Note that the power in the asymptotic behavior in Eq. (25) varies continuously with ε but does not depend on μ.

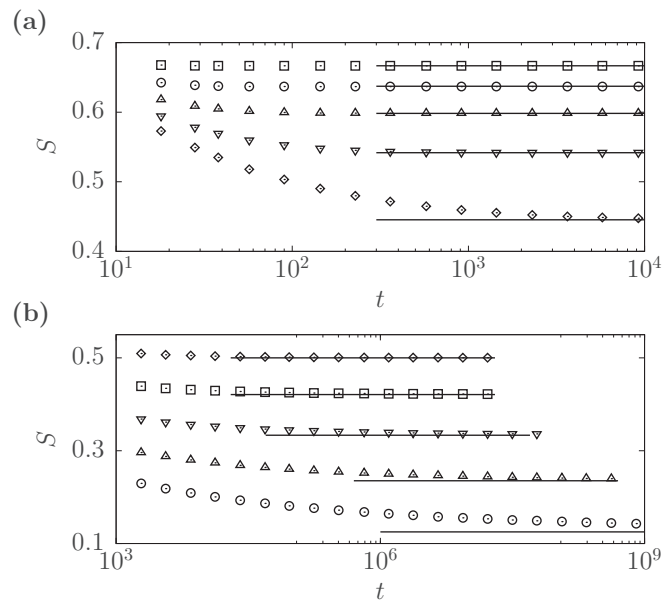

FIG. 1. (a) Plots of S vs t for $\sigma = 0$ (square), 0.2 (circle), 0.4 (up-triangle), 0.6 (down-triangle), and 0.8 (diamond), top to bottom, on a semilogarithmic scale. Here $\varepsilon = 0.5$ and $\mu = 0$. Hoizontal line segments show the value of P_s numerically obtained from Eq. (17). (b) Semilogarithmic plots of S vs t for $\sigma = \mu = 1$ and for $\varepsilon = 0.6$ (circle), 0.7 (up-triangle), 0.8 (down-triangle), 0.9 (square), and 1 (diamond), bottom to top. Hoizontal line segments indicate the predicted P_s in Eq. (24).

For $0 < \sigma < 1$, we show in Appendix A that G_n converges as $n \to \infty$ as long as $\varepsilon > 0$. Hence, we conclude that P_s for any positive ε is nonzero if σ is strictly smaller than 1. Appendix A also shows that G_n diverges as $n \to \infty$ for any ε if $\sigma > 1$, which amounts to $P_s = 0$. Defining the threshold value as $\varepsilon_{\rm th} \equiv \sup\{\varepsilon | P_s = 0\}$, we obtain

$$\varepsilon_{\rm th} = \begin{cases} 0, & \sigma < 1, \\ 1/2, & \sigma = 1, \\ \infty, & \sigma > 1. \end{cases} \tag{26}$$

To confirm, we compare Monte Carlo simulation results with the predictions. Figure 1(a) compares the simulation results for $\sigma < 1$ to the corresponding prediction to show perfect agreement. In Fig. 1(b), we present the simulation results for $\sigma = 1$ and $2\varepsilon > 1$ to find that P_s in Eq. (24) is in perfect agreement with simulations in the long-time limit.

We now present an approximate expression for G_n. Since we are mainly interested in how G_n behaves for large n, we expect that the main contribution of the sum in Eq. (17) occurs when i is large. Accordingly, we have an approximation

$$G_n \approx \int_1^n dx e^{-2\varepsilon I(x;\sigma)}, \quad I(x;\sigma) \equiv \int_{1+\mu}^{x+\mu} y^{-\sigma} dy, \tag{27}$$

where we used $\ln[(1-x)/(1+x)] \simeq -2x$ and replaced sums with integrals.

For $\sigma > 1$, $I(x;\sigma)$ converges as $x \to \infty$, which yields $G_n \sim n$ for any ε, as also shown in Appendix A. Since $G_n = n$ for $\varepsilon = 0$ (unbiased case), we conclude that the case with $\sigma > 1$ shares the universal asymptotic behavior with the unbiased

random walk. We will arrive at the same conclusion when we discuss the asymptotic behavior of $R(t)$ and $S(t)$.

Since $I(x;\sigma) \sim x^{1-\sigma}$ for $\sigma < 1$, G_n for $\varepsilon > 0$ is bounded as expected. For $\varepsilon < 0$, we obtain the asymptotic behavior of $F_1(r)$ as

$$F_1(r) = G_r^{-1} \sim r^{-\sigma} \exp\left(-\frac{2|\varepsilon|}{1-\sigma} r^{1-\sigma}\right), \tag{28}$$

where we have used Eq. (B5) in Appendix B. For $\sigma = 1$, one can easily check that Eq. (27) gives the same asymptotic behaviors as Eqs. (21) and (25).

Now we will find the asymptotic behaviors of $R(t)$ and $S(t)$. Our analysis of $R(t)$ begins with writing down an equation for $R(t)$. Using the master equation (8), we get

$$\frac{dR}{dt} = \varepsilon \sum_{n=1}^{\infty} (n+\mu)^{-\sigma} \psi_n(t) - R(t) \frac{d \ln S(t)}{dt}, \tag{29}$$

where $\psi_n(t) \equiv P_n(t)/S(t)$ with $\sum_{n=1}^{\infty} \psi_n(t) = 1$. If we define $u(t) = R(t)S(t)$, then we get

$$\frac{du}{dt} = \varepsilon S(t) \sum_{n=1}^{\infty} (n+\mu)^{-\sigma} \psi_n(t). \tag{30}$$

Actually, $u(t)$ is the mean distance from the wall to the walker that is averaged over *all* ensemble at time t.

We find a formal solution for $\sigma = 0$ as

$$R(t;\sigma=0) = \frac{1}{S(t)}\left[R_0 + \varepsilon \int_0^t S(t')dt'\right], \tag{31}$$

where R_0 is a constant determined by the initial condition ($R_0 = 1$ for the two-particle initial condition). Since $S(t)$ saturate to nonzero P_s for positive ε, we find

$$R(t;\sigma=0) \sim \varepsilon t. \tag{32}$$

Since $S(t) \sim t^{-1/2}$ for $\varepsilon = 0$ (see, for example, Ref. [34]), we get $R(t;\varepsilon=0) \sim t^{1/2}$.

As we have shown above, $S(t)$ converges to nonzero P_s if $\sigma < 1$ with positive ε or if $\sigma = 1$ with $2\varepsilon > 1$. In these cases, we can neglect the second term in the long-time limit and we have

$$\frac{dR}{dt} \approx \varepsilon \sum_n (n+\mu)^{-\sigma} \psi_n(t), \tag{33}$$

which suggests that $R(t)$, not surprisingly, should increase indefinitely. To find the asymptotic behavior of $R(t)$ for nonzero P_s, let us assume that $\psi_n(t)$ is sharply peaked around $n = R(t)$. Under this assumption, we can approximate the summation in Eq. (33) as (we neglect μ because R is large)

$$\sum_n \frac{\psi_n(t)}{(R+\Delta n)^\sigma} \approx \frac{1}{R^\sigma}\left[1 + \frac{\sigma(\sigma+1)}{2R^2}\langle(\Delta n)^2\rangle_s\right], \tag{34}$$

where $R = \langle n\rangle_s$, $\Delta n \equiv n - R$, and $\langle\cdots\rangle_s$ stands for the average over ψ_n. Hence, we have an approximate equation for $R(t)$ as

$$\frac{dR}{dt} \approx \frac{\varepsilon}{R^\sigma}\left[1 + \frac{\sigma(\sigma+1)}{2}\frac{\langle(\Delta n)^2\rangle_s}{R^2}\right]. \tag{35}$$

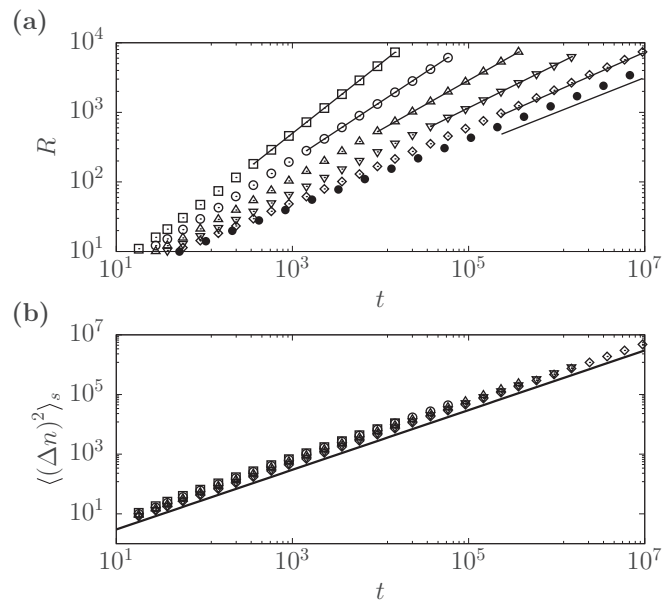

FIG. 2. (a) Double logarithmic plots of R vs t for $\sigma = 0$ (square), 0.2 (circle), 0.4 (up-triangle), 0.6 (down-triangle), 0.8 (diamond), and 1 (filled circle), top to bottom. Here $\varepsilon = 0.5$ for all cases, but $\mu = 0$ for $\sigma < 1$ as in Fig. 1(a) and $\mu = 1$ for $\sigma = 1$ as in Fig. 1(b). Line segments depicts the predicted asymptotic behavior (36), which shows perfect agreement for $\sigma < 1$. The deviation for $\sigma = 1$ is discussed in the text. (b) Double logarithmic plots of $\langle(\Delta n)^2\rangle_s$ vs t for $\sigma = 0$ (square), 0.2 (circle), 0.4 (up-triangle), 0.6 (down-triangle), and 0.8 (diamond). A straight line with slope 1 is drawn for guides to the eyes.

Neglecting the fluctuation $(\Delta n)^2$, we obtain

$$\frac{dR}{dt} \approx \varepsilon R^{-\sigma} \to R \approx [\varepsilon(1+\sigma)t]^{1/(1+\sigma)}, \tag{36}$$

which reproduces the exact asymptotic behavior (32) for $\sigma = 0$.

Now we argue that keeping only the leading term gives the exact asymptotic behavior for $\sigma < 1$ and $\varepsilon > 0$. A (naive) continuum limit for the master equation yields the Fokker-Planck equation

$$\frac{dP(x;t)}{dt} = -\frac{\partial}{\partial x}\left[\frac{\varepsilon}{x^\sigma}P(x;t)\right] + \frac{1}{2}\frac{\partial^2}{\partial x^2}P(x;t), \tag{37}$$

where x is the continuum version of the site index and we neglect μ, assuming x is large. Since the diffusion term in Eq. (37) does not depend on ε, we expect that the variance of x increases linearly just like the unbiased random walks. Accordingly, $\langle\Delta n^2\rangle_s/R^2 \to 0$ as $t \to 0$ for $\sigma < 1$ and, in turn, the approximation (36) becomes accurate in the long-time limit; see Ref. [33] for a similar discussion with negative ε.

We compare Eq. (36) with numerical simulations in Fig. 2(a). Our prediction is in full accord with the simulation results for $\sigma < 1$ and $\varepsilon > 0$. We also measured the fluctuations in simulations to find that it indeed behaves as $\langle(\Delta n)^2\rangle_s \sim t$ for $\sigma < 1$; see Fig. 2(b).

In Fig. 2(a), we also present simulation results for $\sigma = 1$ and $2\varepsilon = 1$ with comparison to Eq. (36). Although the power is still consistent with the prediction, the coefficient deviates

from the prediction. Since $R^2 \sim \langle(\Delta n)^2\rangle_s \sim t$ for $\sigma = 1$ (and $2\varepsilon > 1$), we cannot simply neglect the fluctuation $(\Delta n)^2$, but it only increases the coefficient, which explains why Eq. (36) lies below the simulation data for $\sigma = 1$ in Fig. 2(a).

Let us continue investigating the case with $\sigma = 1$ for arbitrary ε. As above, we begin with writing down an approximate equation for $R(t)$ as

$$\frac{dR}{dt} \approx \frac{\varepsilon}{R} - \frac{d\ln S(t)}{dt}R, \tag{38}$$

where we again neglected the fluctuation. For later purposes, we also write down an approximate equation for u,

$$\frac{du^2}{dt} \approx 2\varepsilon S(t)^2. \tag{39}$$

Notice that Eq. (39) again predicts $R \sim u \sim \sqrt{t}$ for $2\varepsilon > 1$, because $S(t)$ in this case saturates to a nonzero value.

Until now, we have investigated the cases with $P_s > 0$. To find S and R for $P_s = 0$, we will use the following relation. If $S(t) \to 0$ while $R(t) \to \infty$, then S and R are related by

$$S(t) \approx F_1(R), \tag{40}$$

because surviving samples typically arrive at $R(t)$ at time t. We will repeatedly use Eq. (40) in what follows. We will find the asymptotic behaviors of S and R for $2\varepsilon \leqslant 1$ in a self-consistent manner. We first assume $0 \leqslant 2\varepsilon < 1$. Since the repulsion gets stronger as ε gets larger, it seems plausible to expect that $R(t)$ should be a nondecreasing function of ε for given t and, in turn, $R(t) \sim \sqrt{t}$ for $\varepsilon \geqslant 0$, because $R(t) \sim \sqrt{t}$ not only for $\varepsilon = 0$ but also for $2\varepsilon > 1$.

Using Eqs (40) and (25) for $0 < 2\varepsilon < 1$, we find

$$S(t) \sim t^{-(1-2\varepsilon)/2}. \tag{41}$$

If we plug Eq. (41) into Eq. (39), then we get $u \sim t^{\varepsilon}$, which consistently gives $R = u/S \sim \sqrt{t}$. Note that $u(t)$ diverges for $0 < 2\varepsilon < 1$ even though $S(t) \to 0$ as $t \to \infty$.

Since $F_1(r) \sim 1/\ln r$ for $2\varepsilon = 1$, Eq. (40) along with Eq. (21) gives

$$S(t) \sim 1/\ln t. \tag{42}$$

Therefore, we get

$$u^2 \sim \int^t \frac{dt}{(\ln t)^2} = \int^x \frac{e^x}{x^2}dx \sim \frac{e^x}{x^2} = \frac{t}{(\ln t)^2}, \tag{43}$$

where we made a change of variables $x = \ln t$ and Eq. (B5) was used. The logarithm correction in u neatly disappears in the leading behavior of $R(t)$ and we get $R(t) \sim \sqrt{t}$ for all positive ε. This is consistent with the numerical observation in Fig. 2(a) and the assumption that $R(t)$ is a nondecreasing function of ε.

For negative ε, Eq. (30) shows that $u(t)$ always decreases regardless of the initial condition, which shows $u(t) \to 0$ as $t \to \infty$. Assuming that Eq. (39) is a valid approximation for negative ε, we get

$$u^2(t) = \int_\infty^t \frac{du^2}{dt'}dt' \approx 2|\varepsilon| \int_t^\infty S(t')^2 dt'. \tag{44}$$

Assuming $R(t) \sim t^{\gamma}$ for negative ε and using Eq. (40), we get

$$S(t) \sim t^{-(1-2\varepsilon)\gamma}, \tag{45}$$

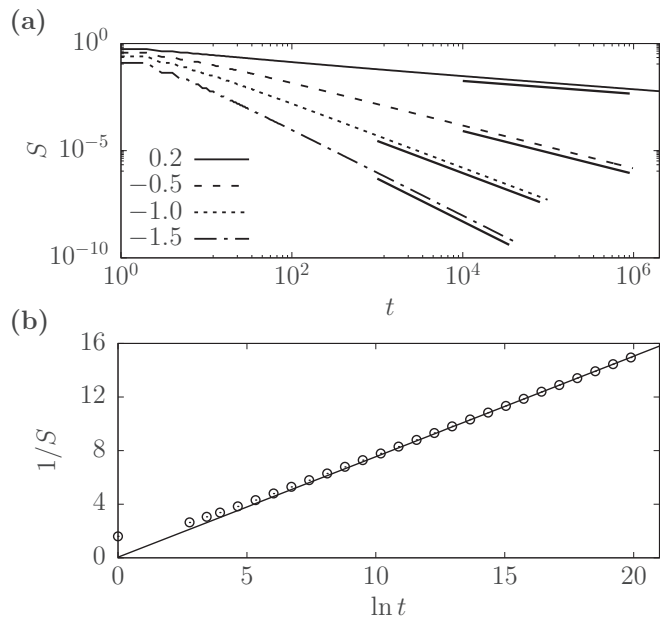

FIG. 3. Survival probability for $\sigma = 1$ and $\mu = 1$. (a) Double logarithmic plots of S vs t for $\varepsilon = 0.2, -0.5, -1$, and -1.5, top to bottom. Line segments with slope $\varepsilon - \frac{1}{2}$ are for guides to the eyes. (b) Plot of $1/S$ vs $\ln t$ for $\varepsilon = 0.5$. The straight line depicts a function $\frac{3}{4}\ln t + a$, where a is determined by a fitting in the region $\ln t \geqslant 16$; see (48).

which together with Eq. (44) gives

$$u(t) \sim t^{-(1-2\varepsilon)\gamma+1/2}. \tag{46}$$

Since $R(t) = u(t)/S(t)$, we get the self-consistent solution $\gamma = 1/2$, that is, $R \sim \sqrt{t}$.

Our findings for $\sigma = 1$ are summarized as

$$R(t) \sim \sqrt{t}, \quad S(t) \sim \begin{cases} (2\varepsilon - 1)/(\mu + \varepsilon), & 2\varepsilon > 1, \\ 1/\ln t, & 2\varepsilon = 1, \\ t^{-(1-2\varepsilon)/2}, & 2\varepsilon < 1. \end{cases} \tag{47}$$

Since $R(t) \sim \sqrt{t}$, neglect of the fluctuation only affects the coefficient and the approximate equation is expected to give the correct power-law behavior.

To support the prediction (47) for $\sigma = 1$, we performed Monte Carlo simulations. In the simulations, we set $\mu = 1$. In Fig. 3(a), we depict $S(t)$ for $\varepsilon = 0.2, -0.5, -1$, and -1.5 on a double logarithmic scale, together with the predicted asymptotic behavior (47) for $2\varepsilon < 1$ as line segments. The prediction perfectly explains the data. For $2\varepsilon = 1$, we put $n \sim \sqrt{t}$ in Eq. (21) to get

$$S(t)^{-1} \sim \tfrac{3}{4}\ln t. \tag{48}$$

In Fig. 3(b), simulation results are compared to the prediction (48) to show excellent agreement.

It is worthwhile to mention that De Coninck *et al.* [35] studied a similar random walk with a reflecting wall at the origin. The hopping probability in Ref. [35] is the same as ours if we set $\sigma = 1$ and $\mu = -\varepsilon = \delta/2$. When the wall at the origin is reflecting, De Coninck *et al.* [35] found $R(t) \sim t^{1-\delta/2}$ for $1 < \delta < 2$, which varies continuously with δ. Since $\mu = -\varepsilon$ in Ref. [35], it is unclear whether the exponent depends on ε

or μ or both. Our results seem to suggest that only ε governs the universal behavior, but detailed analyses are requested for further understanding of the random walk with the reflecting wall, which is beyond the scope of the present paper.

Since $R(t) \sim \sqrt{t}$ if $\sigma = 1$ or if $\sigma = \infty$, it is natural to expect that $R(t) \sim \sqrt{t}$ for any $\sigma > 1$. In this case, the term with $R^{-\sigma}$ in Eq. (36) is negligible and we get $S(t) \sim R(t) \sim t^{-1/2}$. Notice that this is also consistent with Eq. (40) because $F_1(r) \sim 1/r$ for $\sigma > 1$. Hence, the bias is immaterial if $\sigma > 1$ and the long-range nature is crucial only when $\sigma \leqslant 1$.

Last, we investigate the case with $\sigma < 1$ and $\varepsilon = -|\varepsilon|$. In Appendix C, we find the exact expression of $P_i(t)$ for $\sigma = 0$, which is

$$P_i(t) = w^{i-1}\frac{2i}{x}I_i(x)e^{-t},\ w \equiv \sqrt{\frac{1+\varepsilon}{1-\varepsilon}}, \tag{49}$$

where $x = t\sqrt{1-\varepsilon^2}$ and $I_i(x)$ is the modified Bessel function of the first kind. Using $I_i(x) \sim e^x/\sqrt{2\pi x}$ for large x, one can readily get

$$\begin{aligned} S(t) &\sim t^{-3/2}\exp[-(1-\sqrt{1-\varepsilon^2})t], \\ \pi_i &\equiv \lim_{t\to\infty}\psi_i(t) = (1-w)^2 i w^{i-1}, \\ \lim_{t\to\infty} R(t) &= \frac{1+w}{1-w} = \frac{1+\sqrt{1-\varepsilon^2}}{|\varepsilon|}. \end{aligned} \tag{50}$$

Note that π_i is the quasistationary distribution in that it is the steady-state solution of the equation

$$\frac{d\psi_i}{dt} = q\psi_{i-1} + (1-q)\psi_{i+1} + [(1-q)\psi_1 - 1]\psi_i, \tag{51}$$

where $\psi_0 = 0$ and $w^2 = q/(1-q)$. For the discrete-time random walk, there is no quasistationary state in that

$$\lim_{m\to\infty}\frac{r_{2m}}{r_{2m-1}} \neq 1, \tag{52}$$

though $\xi_{2m-1} = \xi_{2m}$ for all $m \geqslant 1$.

Since $F_1(r)$ decays exponentially for $\sigma < 1$, it is plausible to anticipate that $S(t)$ also decays exponentially in the form $S(t) \sim t^{-\alpha}\exp(-\lambda t^\beta)$. If we further assume $\langle (n+\mu)^{-\sigma}\rangle_s \sim t^{-\eta}$, then Eq. (30) gives

$$\begin{aligned} u(t) &= |\varepsilon|\int_t^\infty S(t')\langle (n+\mu)^{-\sigma}\rangle_s dt' \\ &\sim \int_t^\infty x^{-\alpha-\eta}\exp(-\lambda x^\beta)dx \\ &\sim \int_{t^\beta}^\infty y^{-1+(1-\alpha-\eta)/\beta}e^{-\lambda y}dy \sim t^{1-\eta-\beta-\alpha}e^{-\lambda t^\beta} \end{aligned} \tag{53}$$

and $R = u/S \sim t^{1-\eta-\beta}$. If a quasistationary state exists, then η must be zero by definition and, in turn, β must be 1. Hence, a quasistationary state cannot exist if $\beta < 1$.

In Fig. 4, we present numerical calculations of $S(t)$ and $R(t)$. As can be seen in Fig. 4(a), β is clearly smaller than 1 for $\sigma > 0$ [a fitting of the data for $\sigma = 0.1$ in Fig. 4(a) gives $\beta \approx 0.8$] and indeed $R(t)$ increases algebraically; see Fig. 4(b). The quasistationary state is a special feature of the case with $\sigma = 0$.

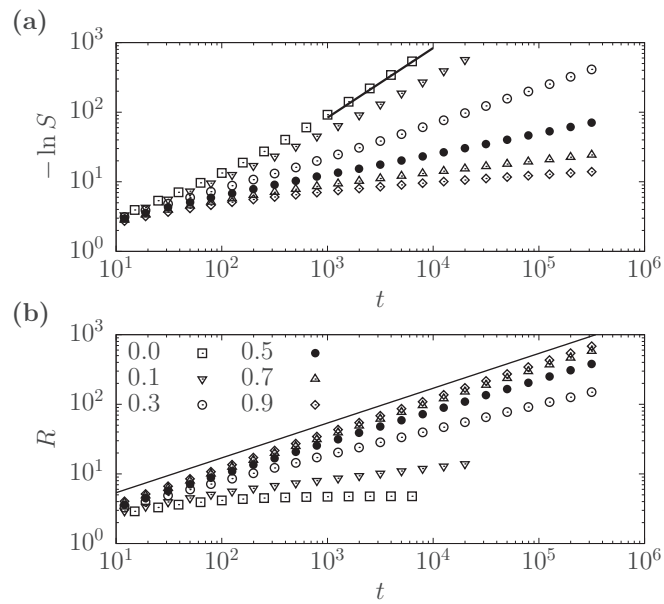

FIG. 4. (a) Double logarithmic plots of $-\ln S$ vs t for $\sigma = 0$, 0.1, 0.3, 0.5, 0.7, and 0.9 (top to bottom) with $\varepsilon = -0.4$ and $\mu = 0$. The line segment depcits the exact asymptotic behavior, $(1-\sqrt{1-\varepsilon^2})t$, for $\sigma = 0$. (b) Double logarithmic plots of R vs t for $\sigma = 0$, 0.1, 0.3, 0.5, 0.7, and 0.9 (bottom to top) with $\varepsilon = -0.4$ and $\mu = 0$. The straight line with slope 0.5 is a guide for the eyes.

Since R increases indefinitely for $0 < \sigma < 1$, we use the same logic as in Eq. (40) to get the self-consistent solution,

$$(1-\eta-\beta)(1-\sigma) = \beta \to \beta = \frac{1-\sigma}{2-\sigma}(1-\eta), \tag{54}$$

$$R \sim t^{(1-\eta)/(2-\sigma)}, \quad \alpha = \frac{\sigma}{2-\sigma}(1-\eta). \tag{55}$$

If we can approximate $\langle (n+\mu)^{-\sigma}\rangle_s \propto R^{-\sigma}$ as before, then the self-consistent argument gives

$$\eta = \frac{\sigma}{2}, \quad R \sim \sqrt{t}, \quad \beta = \frac{1-\sigma}{2}, \tag{56}$$

which cannot be consistent with Fig. 4(a), especially for small σ. Hence, the mean-field-like approximation $\langle (n+\mu)^{-\sigma}\rangle_s \propto R^{-\sigma}$ does not work in this case. Still, Eq. (56) gives a reasonably good approximation for large σ. It seems challenging to find the correct asymptotic behavior for $0 < \sigma < 1$ and $\varepsilon < 0$, which is deferred to a later publication.

IV. BEHAVIOR OF THE DENSITY

With the two-particle initial condition, the direction of the bias does not change and the particles can survive forever with nonzero probability P_s, once the repulsion is strong. When the density is finite, however, a particle should meet another particle and is annihilated almost surely even if P_s is nonzero and the system size is infinite. Hence the asymptotic behavior of the density cannot be directly explained by the results in Sec. III. The purpose of this section is to investigate how the density $\rho(t)$ decreases if the system evolves from the fully occupied initial condition.

Assume that there are $N = \rho L$ particles at time t. Here ρ is assumed small. The site index of the kth particle is denoted by n_k ($k = 1, \ldots, N$, $n_1 < n_2 < \cdots < n_N$). The mean distance between the kth and $(k+1)$st particles is $\langle n_{k+1} - n_k \rangle = 1/\rho$ and the variance is expected to be $\langle (n_{k+1} - n_k - 1/\rho)^2 \rangle \sim 1/\rho$ (as we will see soon, the exact form of the variance is immaterial as long as its square root is much smaller than $1/\rho$).

When ρ is small, a (mean) time gap between any two consecutive pair-annihilation events within a region of size $O(1/\rho)$ is expected to be large. Assume that the kth particle is to be annihilated. As an approximation, we assume that only the kth particle performs random walks and all other particles remain still before the kth particle is annihilated. Under this approximation, dynamics of the kth particle can be mapped to a random-walk problem with two walls, one of which is reflecting and the other is absorbing.

To be concrete, let $n_k = \ell$, $n_{k-1} = -r$, and $n_{k+1} = r$, where $|r - 1/\rho| = O(1/\sqrt{\rho})$ and $\ell = O(1/\sqrt{\rho})$. Within the approximation, n_{k+1} and n_{k-1} do not change and n_k changes according to the rule in Eq. (2). Since the dynamics are invariant under the transformation $\ell \mapsto -\ell$ and $n_{k+1} \leftrightarrow n_{k-1}$, we can set $\ell \geqslant 0$ without loss of generality and we can treat the origin as a reflecting wall and site r as an (immovable) absorbing wall. In the following, we will call the kth particle the walker.

This random-walk problem can be formulated as follows. Let $H_i(t)$ be the probability that the walker is located at site i at time t and $H_i(0) = \delta_{i,\ell}$. The time t here should not be confused with the time that appeared in the beginning of this section. We write the master equation ($0 \leqslant i \leqslant r$)

$$\frac{dH_i(t)}{dt} = b_{i-1}H_{i-1} + d_{i+1}H_{i+1} - (1 - \delta_{r,i})H_i, \tag{57}$$

where $b_0 = 1$, $b_{-1} = d_0 = d_{r+1} = 0$, and ($0 < k < r$),

$$b_k = \frac{1}{2} - \frac{\varepsilon}{2}(r - k + \mu)^{-\sigma}, \quad d_k = 1 - b_k. \tag{58}$$

Recall that the absorbing wall is a particle in the AWL; it exerts repulsive (attractive) interaction to the walker if ε is positive (negative). We are interested in the mean first-passage time, to be denoted by $\tau(\rho)$, for the walker to reach the absorbing wall.

Since $2/\tau(\rho)$ can be interpreted as a rate of removal per particle in the AWL (the factor 2 is multiplied because of the pair annihilation, but this factor does not affect the universal behavior that we will find), the behavior of $\rho(t)$ can be analyzed by the equation

$$\frac{d\rho}{dt} \propto -\frac{\rho}{\tau(\rho)}. \tag{59}$$

If we find $\tau(\rho)$, then we can obtain the asymptotic behavior of $\rho(t)$. One can use Eq. (59) even if the particles perform coalescing random walks ($A + A \to A$).

Let T_i be the mean first-passage time if the walker starts from site i at $t = 0$. By definition, we have $T_r = 0$. We will approximate $\tau(\rho)$ as T_ℓ with $\ell = O(1/\sqrt{\rho})$. Due to the Markov property, we have the recursion relation

$$T_i = 1 + b_i T_{i+1} + d_i T_{i-1}. \tag{60}$$

In other words, the walker waits unit time on average and then jumps to site $i+1$ ($i-1$) with probability b_i (d_i), after which it should spend T_{i+1} (T_{i-1}).

To find a formal solution, we define $\chi_i \equiv T_i - T_{i+1}$ and we rewrite Eq. (60) as

$$\chi_i = \frac{d_i}{b_i}\chi_{i-1} + \frac{1}{b_i}. \tag{61}$$

Multiplying Eq. (61) by $\prod_{k=1}^{i}(b_k/d_k)$, we get

$$\chi_i \prod_{k=1}^{i} \frac{b_k}{d_k} - \chi_{i-1} \prod_{k=1}^{i-1} \frac{b_k}{d_k} = \frac{1}{d_i} \prod_{k=1}^{i-1} \frac{b_k}{d_k}, \tag{62}$$

where we assume $\prod_{k=1}^{0} \equiv 1$. After a little algebra, we have

$$\chi_{r-n} = \prod_{k=n}^{r-1} \frac{d_{r-k}}{b_{r-k}} + \sum_{j=n}^{r-1} \frac{1}{d_{r-j}} \prod_{k=n}^{j} \frac{d_{r-k}}{b_{r-k}}. \tag{63}$$

Since $T_r = 0$, we can write

$$T_i = \sum_{n=i}^{r-1} \chi_n = \sum_{n=1}^{r-i} \chi_{r-n}, \tag{64}$$

which gives

$$T_i = \sum_{n=1}^{r-i} \sum_{j=n}^{r-1} \left(\delta_{j,r-1} + \frac{1}{d_{r-j}} \right) \prod_{k=n}^{j} \frac{d_{r-k}}{b_{r-k}} \tag{65}$$

for $i \geqslant 1$ and $T_0 = 1 + T_1$.

For certain cases, we find a simple expression of T_0. For $\varepsilon = 0$ (or equivalently $\sigma = \infty$ with $\mu > 0$) one can readily get $T_0 = r^2$. For later purposes, we write

$$T_0(\sigma = \infty) \sim r^2. \tag{66}$$

For $\sigma = 0$, it is straightforward to get

$$T_0(\sigma = 0) = \frac{1 - \varepsilon^2}{2\varepsilon^2} \left[\left(\frac{1+\varepsilon}{1-\varepsilon} \right)^r - 1 \right] - \frac{r}{\varepsilon}. \tag{67}$$

If ε is positive, then T_0 grows exponentially with r. If ε is negative, then $T_0 \sim r$ for large r.

By definition, T_i cannot be smaller than $r - i$, so T_i for any case increases indefinitely with r as long as $i \ll r$. Considering $0 < 1 - |\varepsilon|(1+\mu)^{-\sigma} < 2d_j < 2$ for all positive j, we can write

$$T_i \sim \sum_{n=1}^{r-i} \sum_{j=n}^{r-1} \prod_{k=n}^{j} \frac{1 + \varepsilon(k+\mu)^{-\sigma}}{1 - \varepsilon(k+\mu)^{-\sigma}}. \tag{68}$$

Since the leading asymptotic behavior of T_i for large r does not depend on i if $i/r \to 0$, it is sufficient to analyze the asymptotic behavior of T_0,

$$T_0 \sim \sum_{i=2}^{r-1} \sum_{n=1}^{i} \prod_{k=n}^{i} \frac{1 + \varepsilon(k+\mu)^{-\sigma}}{1 - \varepsilon(k+\mu)^{-\sigma}}, \tag{69}$$

where we replaced the dummy index j with i and we changed the order of the summations. For convenience, we neglect the contribution from $i = 1$, which does not have r dependence. In the following three subsections, we will study the AWL for three different cases: $\sigma < 1$, $\sigma = 1$, and $\sigma > 1$.

A. $0 < \sigma < 1$

Since T_0 diverges with r, the dominant contribution to T_0 should arise for large k in Eq. (69). Accordingly, we approximate the product in Eq. (69) as

$$\prod_{k=n}^{i} \frac{1+\varepsilon(k+\mu)^{-\sigma}}{1-\varepsilon(k+\mu)^{-\sigma}} \approx \exp\left(\int_{n+\mu}^{i+\mu} 2\varepsilon k^{-\sigma} dk\right). \tag{70}$$

Approximating the summations in Eq. (69) by integrals as well, we get

$$T_0 \sim \int_2^{r-1} dx e^{f(x+\mu)} \int_1^x dn e^{-f(n+\mu)}, \tag{71}$$

where $f(x) = C_\sigma x^{1-\sigma}$ with $C_\sigma = 2\varepsilon/(1-\sigma)$. Since, for $\varepsilon > 0$ ($C_\sigma > 0$) and $x \geqslant 2$,

$$\begin{aligned}\int_1^2 dn e^{-f(n+\mu)} &\leqslant \int_1^x dn e^{-f(n+\mu)} \\ &\leqslant \int_0^\infty dn e^{-f(n)} = C_\sigma^{1/(\sigma-1)} \Gamma\left(\frac{2-\sigma}{1-\sigma}\right),\end{aligned} \tag{72}$$

we get

$$T_0 \sim \int_1^{r-1} \exp(C_\sigma x^{1-\sigma}) dx \sim r^\sigma \exp(C_\sigma r^{1-\sigma}), \tag{73}$$

where we have used Eq. (B5).

For negative ε ($C_\sigma < 0$), the integral with variable n in Eq. (71) diverges as $x \to \infty$. We again use Eq. (B5) to get

$$T_0 \sim \int_1^{r-1} x^\sigma dx \sim r^{1+\sigma}. \tag{74}$$

To summarize, we obtain

$$T_0 \sim \begin{cases} r^\sigma \exp(C_\sigma r^{1-\sigma}), & \varepsilon > 0, \\ r^{1+\sigma}, & \varepsilon < 0, \end{cases} \tag{75}$$

where μ does not play any role. Note that Eq. (75) reproduces the exact result for $\sigma = 0$ if we set $C_0 = \ln(1+\varepsilon) - \ln(1-\varepsilon)$. Although we arrive at Eq. (75) by an approximation, this result is actually exact when it comes to the leading asymptotic behavior.

Now we investigate the long-time behavior of the AWL by analyzing Eq. (59) with $\tau(\rho) = T_0(1/\rho)$. For $0 \leqslant \sigma < 1$ and $\varepsilon > 0$, we have

$$\frac{d\rho}{dt} \sim -\rho^{1+\sigma} e^{-C_\sigma \rho^{-1+\sigma}}, \tag{76}$$

which can be solved approximately for small ρ (for large t) as

$$\begin{aligned} t(\rho) &\sim \int_\rho^1 \rho^{-1-\sigma} \exp(C_\sigma \rho^{-1+\sigma}) d\rho \\ &= \int_1^{1/\rho} x^{\sigma-1} \exp(C_\sigma x^{1-\sigma}) dx \\ &\sim \rho^{1-2\sigma} \exp(C_\sigma \rho^{-1+\sigma}), \end{aligned} \tag{77}$$

where we have used Eq. (B5). Here

$$C_\sigma = \begin{cases} 2\varepsilon/(1-\sigma), & \sigma > 0, \\ \ln[(1+\varepsilon)/(1-\varepsilon)], & \sigma = 0. \end{cases} \tag{78}$$

Accordingly, we get

$$\begin{aligned} \rho(t) &\sim [\ln t - (1-2\sigma)\ln\rho]^{-1/(1-\sigma)} \\ &\sim (\ln t)^{-1/(1-\sigma)}. \end{aligned} \tag{79}$$

To confirm the prediction, we performed Monte Carlo simulations for $\sigma = 0, 0.2, 0.5$ and 0.8 with system size $L = 2^{22}$ ($\sigma = 0$) or $L = 2^{20}$ ($\sigma \geqslant 0.2$). In Fig. 5, we compare simulation results with Eq. (77). Our prediction is in excellent agreement with simulations up to nonuniversal multiplication factors.

Before closing this subsection, we consider the case with negative ε. Since $\tau(\rho) \sim \rho^{-1-\sigma}$ for $0 \leqslant \sigma < 1$, we get

$$\frac{d\rho}{dt} \sim -\rho^{2+\sigma} \to \rho \sim t^{-1/(1+\sigma)}, \tag{80}$$

which was already confirmed numerically in Ref. [33]; see also Eq. (4).

B. AWL for $\sigma = 1$

Since Eq. (79) breaks down when $\sigma = 1$, we treat the case with $\sigma = 1$ separately in this subsection. Using the approximation (70), we get

$$\prod_{k=n}^{i} \frac{1+\varepsilon(k+\mu)^{-1}}{1-\varepsilon(k+\mu)^{-1}} \sim \left(\frac{i+\mu}{n+\mu}\right)^{2\varepsilon}, \tag{81}$$

which gives

$$\begin{aligned} T_0 &\sim \int^r dx (x+\mu)^{2\varepsilon} \int_1^x (n+\mu)^{-2\varepsilon} dn \\ &\sim \begin{cases} r^2, & 2\varepsilon < 1, \\ r^2 \ln r, & 2\varepsilon = 1, \\ r^{1+2\varepsilon}, & 2\varepsilon > 1. \end{cases} \end{aligned} \tag{82}$$

As in Sec. III, a logarithmic behavior appears for $2\varepsilon = 1$.

Actually, we found exact expressions of T_0 for $\sigma = 1$. For $2\varepsilon = 1$, we find

$$T_0 = r + 2\sum_{n=1}^{r}\sum_{i=n}^{r-1} \frac{2i+2\mu-1}{2n+2\mu-1} \sim r^2 \ln r, \tag{83}$$

and for $2\varepsilon \neq 1$

$$\begin{aligned} T_0 = &\frac{2\Gamma(\mu+1-\varepsilon)}{(4\varepsilon^2-1)\Gamma(\mu+\varepsilon)} \frac{\Gamma(r+\mu+1+\varepsilon)}{\Gamma(r+\mu-\varepsilon)} \\ &+ \frac{r^2+2\mu r+2(\mu^2-\varepsilon^2)/(1+2\varepsilon)}{1-2\varepsilon}, \end{aligned} \tag{84}$$

where we have repeatedly used Eq. (22). Using the Stirling's formula, one can arrive at Eq. (82).

Equations (59) and (82) now yield

$$\frac{d\rho}{dt} \sim \begin{cases} -\rho^3, & 2\varepsilon < 1 \\ \rho^3/\ln\rho, & 2\varepsilon = 1, \\ -\rho^{2+2\varepsilon}, & 2\varepsilon > 1, \end{cases} \tag{85}$$

whose solutions are

$$t \sim \begin{cases} \rho^{-2}, & 2\varepsilon < 1 \\ -\ln\rho/\rho^2, & 2\varepsilon = 1, \\ \rho^{-1-2\varepsilon}, & 2\varepsilon > 1. \end{cases} \tag{86}$$

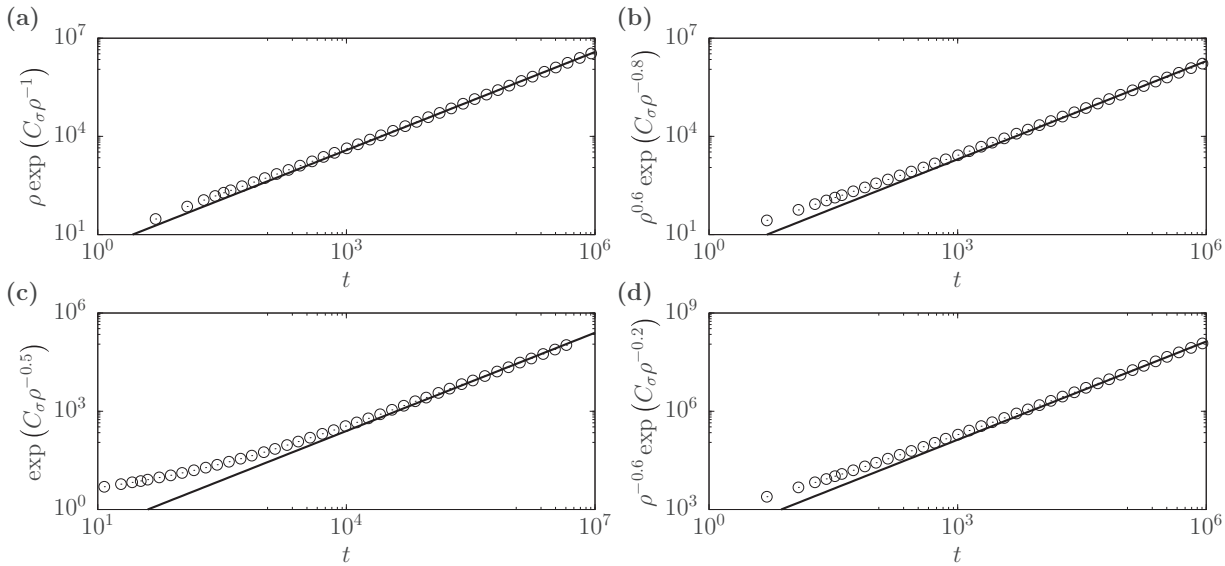

FIG. 5. Double logarithmic plots of $\rho^{1-2\sigma} \exp\left(C_\sigma \rho^{-1+\sigma}\right)$ vs t for (a) $\sigma = 0$, $\varepsilon = \frac{1}{2}$ ($C_\sigma = \ln 3$), (b) $\sigma = 0.2$, $\varepsilon = \frac{1}{2}$ ($C_\sigma = 1.25$), (c) $\sigma = 0.5$, $\varepsilon = \frac{1}{8}$ ($C_\sigma = 0.5$), (d) $\sigma = 0.8$, $\varepsilon = \frac{1}{2}$ ($C_\sigma = 5$); see Eq. (77). For guides to the eyes, we also draw a straight line with slope 1 in each panel.

Inverting the function, we get the asymptotic behavior of ρ as

$$\rho \sim \begin{cases} t^{-1/2}, & 2\varepsilon < 1 \\ \sqrt{\ln t/t}, & 2\varepsilon = 1, \\ t^{-1/(1+2\varepsilon)}, & 2\varepsilon > 1. \end{cases} \tag{87}$$

Now we present our simulation results for four cases with $\varepsilon = \frac{1}{4}$ ($L = 2^{22}$), $\varepsilon = \frac{1}{2}$ ($L = 2^{22}$), $\varepsilon = 1$ ($L = 2^{22}$), and $\varepsilon = 2$ ($L = 2^{21}$). We use $\mu = 2$ for $\varepsilon \geqslant 1$ and $\mu = 0$ for $\varepsilon < 1$. The simulation results are presented in Fig. 6. The long-time behavior is in excellent agreement with our prediction up to nonuniversal multiplication constants.

C. AWL for $\sigma > 1$

Since

$$\ln \frac{1+\varepsilon x}{1-\varepsilon x} \leqslant x \ln \frac{1+\varepsilon}{1-\varepsilon} \tag{88}$$

for $0 < \varepsilon < 1$ and

$$\ln \frac{1+\varepsilon x}{1-\varepsilon x} \leqslant 2\varepsilon x \tag{89}$$

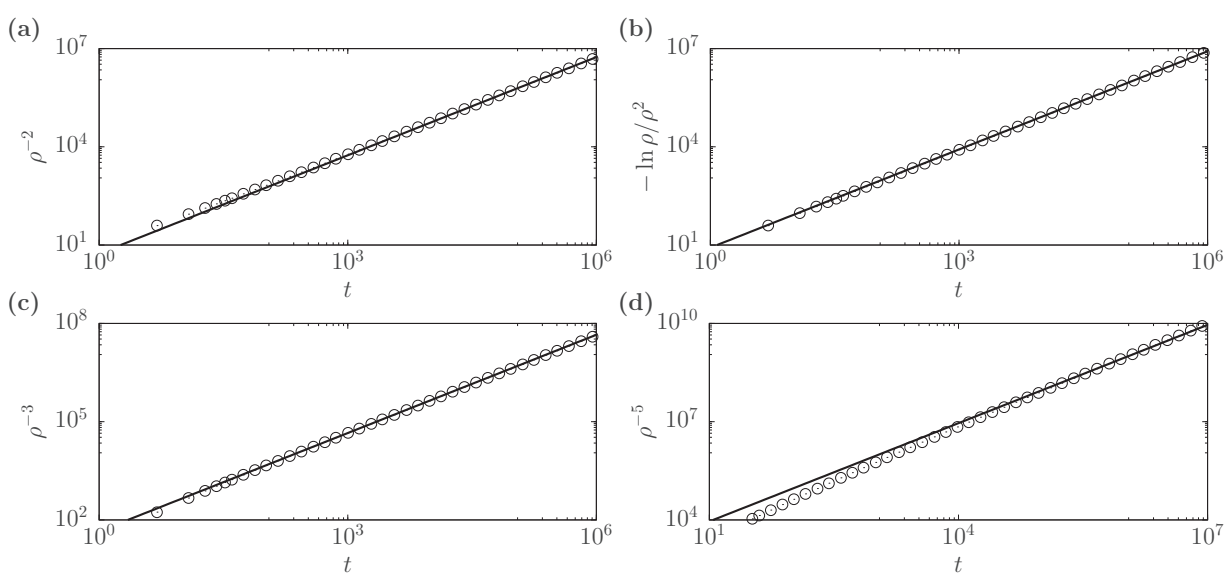

FIG. 6. Behavior of density of the AWLR with $\sigma = 1$ on a double-logarithmic scale. (a) ρ^{-2} vs t for $\varepsilon = \frac{1}{4}$. (b) $-\ln \rho/\rho^2$ vs t for $\varepsilon = \frac{1}{2}$. (c) ρ^{-3} vs t for $\varepsilon = 1$. (c) ρ^{-5} vs t for $\varepsilon = 2$. For guides to the eyes, we also draw a straight line with slope 1 in each panel.

TABLE I. The asymptotic behaviors of $R(t)$, $S(t)$, and $\rho(t)$ for $\sigma \leqslant 1$.

	$\sigma = 1$			$\varepsilon > 0$	$\varepsilon < 0$	
	$2\varepsilon > 1$	$2\varepsilon = 1$	$2\varepsilon < 1$	$0 \leqslant \sigma < 1$	$\sigma = 0$	$0 < \sigma < 1$ [a]
$R(t)$	$\sqrt{t}$	$\sqrt{t}$	$\sqrt{t}$	$t^{1/(1+\sigma)}$	Constant	t^{γ}
$S(t)$	Constant	$(\ln t)^{-1}$	$t^{-(1-2\varepsilon)}$	Constant	$t^{-3/2}\exp[-(1-\sqrt{1-\varepsilon^2})t]$	$t^{-\alpha}\exp[-\lambda t^{\beta}]$
$\rho(t)$	$t^{-1/(1+2\varepsilon)}$	$\sqrt{\ln t/t}$	$t^{-1/2}$	$(\ln t)^{-1/(1-\sigma)}$	t^{-1}	$t^{-1/(1+\sigma)}$

[a] $\gamma > 0$ and $0 < \beta < 1$. Exact formulas for α, β, γ, and λ are not available in this work.

for $-1 < \varepsilon < 0$, where $0 < x < 1$, we have an inequality

$$\prod_k \frac{1+\varepsilon(k+\mu)^{-\sigma}}{1-\varepsilon(k+\mu)^{-\sigma}} \leqslant \exp\left[D_\varepsilon \sum_{k=1}^{\infty}(k+\mu)^{-\sigma}\right] \leqslant \exp\left[D_\varepsilon \sum_{k=1}^{\infty} k^{-\sigma}\right] = \exp\left[D_\varepsilon \zeta(\sigma)\right], \tag{90}$$

where $\zeta(\sigma)$ is the Riemann zeta function ($\sigma > 1$) and

$$D_\varepsilon = \begin{cases} \ln[(1+\varepsilon)/(1-\varepsilon)], & \varepsilon > 0, \\ 2\varepsilon, & \varepsilon < 0. \end{cases} \tag{91}$$

Thus, T_0 is bounded by a square function of r.

Since T_0 for given r is an increasing (a decreasing) function of σ for negative (positive) ε, we have a lower bound,

$$T_0(\sigma > 1) \geqslant \begin{cases} T_0(\sigma = \infty) \sim r^2, & \varepsilon > 0, \\ T_0(\sigma = 1) \sim r^2, & \varepsilon < 0. \end{cases} \tag{92}$$

Therefore, we get $T_0 \sim r^2$ for any ε if $\sigma > 1$ and the AWL with $\sigma > 1$ shares the (universal) long-time behavior with the annihilating random walk without bias. The same conclusion was arrived at in Sec. III.

V. SUMMARY AND DISCUSSION

We have studied the annihilating random walk with long-range interaction in one dimension. The long-range interaction manifests its presence by the hopping bias in the transition rate (2). We have investigated the survival probability $S(t)$ and the mean spreading $R(t)$ of surviving samples for the two-particle initial condition and the density ρ for the fully occupied initial condition. The results for $\sigma \leqslant 1$ are summarized in Table I.

For $\sigma > 1$, the system turned out to show the same universal behavior as the unbiased annihilating random walk, which was already anticipated in Ref. [33] for the AWLA.

For $\sigma < 1$, the sign of ε plays an important role. When $\varepsilon > 0$ (AWLR), we have found that $S(t)$ saturates to a nonzero value, a mean-field-like approximation gives the exact asymptotic behavior of $R(t)$, and $\rho(t)$ decays logarithmically. When $\varepsilon < 0$ (AWLA), the mean-field-like approximation failed to predict the right asymptotic behavior for $R(t)$ and $S(t)$ for $0 < \sigma < 1$. We only reported the numerical results. But, when $\sigma = 0$ and $\varepsilon < 0$, the exact asymptotic behaviors of $R(t)$ and $S(t)$ are available. Actually, there is a quasistationary state in this case.

For $\sigma = 1$, the threshold value of ε is shifted to $\frac{1}{2}$. When $2\varepsilon > 1$, $S(t)$ saturates to a nonzero value, while $\rho(t)$ decays with continuously varying exponent that depends on ε. When $2\varepsilon < 1$, $S(t)$ decays with continuously varying exponent with ε, while $\rho(t)$ shows a universal behavior. When $2\varepsilon = 1$, $S(t)$ decays logarithmically and $\rho(t)$ has a logarithmic correction. In all cases, $R(t)$ shows the universal $\sqrt{t}$ behavior.

In a different context, continuously varying decaying exponent in coarsening dynamics was observed in Refs. [36,37]. We hope our results shed some light on deeper understanding of the coarsening dynamics in Refs. [36,37].

For the unbiased case, the annihilating random walk was analyzed by the RG [8,12]. It would be an intriguing task to analyze the AWL by the RG, because the long-range interaction would appear as a multiplication of many fields in field-theoretical action.

When branching is introduced to the AWLA, rich critical phenomena have been reported especially for the case of the even number of offspring [33,38,39]. In this context, it is natural to ask what would happen if branching is introduced to the AWLR. If we think naively, then we would conclude that as soon as branching is introduced, the steady-state density is nonzero for $\sigma < 1$ and $\varepsilon > 0$, because P_s is nonzero for $\sigma < 1$ in the AWLR. Our preliminary studies show, however, that this scenario is not true in general and the branching actually triggers rich phenomena. These results will be published elsewhere.

ACKNOWLEDGMENTS

This work was supported by the National Research Foundation of Korea (NRF) grant funded by the Korea government (MSIT) (Grant No. 2020R1F1A1077065) and by the Catholic University of Korea, research fund 2020. The author furthermore thanks the Regional Computing Center of the University of Cologne (RRZK) for providing computing time on the DFG-funded High Performance Computing (HPC) system CHEOPS.

APPENDIX A: CONVERGENCE OR DIVERGENCE OF G_n

In this Appendix, we prove that G_n defined in Eq. (17) converges as $n \to \infty$ if $\sigma < 1$ and $\varepsilon > 0$ and diverges if $\sigma > 1$.

We first consider the case with $\sigma < 1$ and $\varepsilon > 0$. Using the inequality ($0 \leqslant y < 1$)

$$\ln \frac{1-y}{1+y} \leqslant -2y, \tag{A1}$$

we get

$$\prod_{k=1}^{i}\frac{1-\varepsilon(k+\mu)^{-\sigma}}{1+\varepsilon(k+\mu)^{-\sigma}} \leqslant \exp\left[-2\varepsilon\sum_{k=1}^{i}(k+\mu)^{-\sigma}\right]. \tag{A2}$$

Since

$$\int_1^i (k+\mu)^{-\sigma}dk \leqslant \sum_{k=1}^{i}(k+\mu)^{-\sigma}, \tag{A3}$$

we have an inequality

$$\prod_{k=1}^{i}\frac{1-\varepsilon(k+\mu)^{-\sigma}}{1+\varepsilon(k+\mu)^{-\sigma}} \leqslant C_1\exp[-C_0(i+\mu)^{1-\sigma}], \tag{A4}$$

where $C_0 = 2\varepsilon/(1-\sigma)$ and $C_1 = \exp[(1+\mu)^{1-\sigma}C_0]$. Since the sum of the right-hand side of Eq. (A4) from $i = 1$ to $i = \infty$ is obviously finite, G_n for positive ε should converge to a finite value as $n \to \infty$.

Now we move on to the case with $\sigma > 1$. Since

$$\ln\frac{1-y}{1+y} \geqslant -2y \tag{A5}$$

for $-1 < y < 0$ and

$$\ln\frac{1-\varepsilon y}{1+\varepsilon y} \geqslant -y\ln\frac{1+\varepsilon}{1-\varepsilon}, \tag{A6}$$

for $0 < y < 1$ and $0 < \varepsilon < 1$, there is a positive C_2 such that

$$\ln\frac{1-\varepsilon(k+\mu)^{-\sigma}}{1+\varepsilon(k+\mu)^{-\sigma}} \geqslant -C_2(k+\mu)^{-\sigma}, \tag{A7}$$

for given ε. Since

$$(1+\mu)^{-\sigma} + \int_1^i (k+\mu)^{-\sigma}dk \geqslant \sum_{k=1}^{i}(k+\mu)^{-\sigma}, \tag{A8}$$

there are positive constants C_3 and C_4 such that

$$\prod_{k=1}^{i}\frac{1-\varepsilon(k+\mu)^{-\sigma}}{1+\varepsilon(k+\mu)^{-\sigma}} \geqslant C_3\exp[-C_4(i+\mu)^{1-\sigma}]. \tag{A9}$$

If $\sigma > 1$, then the lower bound of Eq. (A9) can be set $C_5 = C_3\exp[-C_4(1+\mu)^{1-\sigma}]$, which gives $G_n \geqslant C_5(n-1)$. Thus, G_n diverges for any ε if $\sigma > 1$. In a similar manner, one can easily show that there is a positive C_6 such that $G_n \leqslant C_6 n$. Hence, $G_n \sim n$ for $\sigma > 1$.

APPENDIX B: ASYMPTOTIC EXPANSION USING INTEGRATION BY PARTS

In this Appendix, we find the leading behavior for large r of the integral (for a general discussion, see, for example, Ref. [40])

$$I_1 \equiv A\alpha\int_1^r x^\beta\exp(Ax^\alpha)dx = A\int_1^{r^\alpha} y^\gamma e^{Ay}dy, \tag{B1}$$

where $\alpha > 0$, $A > 0$, and $\gamma = (1+\beta-\alpha)/\alpha$. By an integration by parts, we get

$$I_1 = r^{1+\beta-\alpha}\exp(Ar^\alpha) - e^A - \gamma I_2, \tag{B2}$$

$$I_2 \equiv \int_1^{r^\alpha} y^{\gamma-1}e^{Ay}dy. \tag{B3}$$

For I_2, we split the integral as

$$\int_1^{r^\alpha/2} y^{\gamma-1}e^{Ay}dy \leqslant \frac{1}{A}\max\left\{1, \left(\frac{r^\alpha}{2}\right)^{\gamma-1}\right\}e^{Ar^\alpha/2},$$

$$\int_{r^\alpha/2}^{r^\alpha} y^{\gamma-1}e^{Ay}dy \leqslant \frac{1}{A}\max\{1, 2^{1-\gamma}\}r^{1+\beta-2\alpha}e^{Ar^\alpha}, \tag{B4}$$

which shows $I_2/I_1 \to 0$ as $r \to 0$. Hence, we get

$$I_1 \sim r^{1+\beta-\alpha}\exp(Ar^\alpha). \tag{B5}$$

APPENDIX C: DERIVATION OF EQ. (49)

In this Appendix, we derive Eq. (49) for $\sigma = 0$. We first find $d_{i,n}$ defined in Eq. (11). Let q be the probability of hopping to the right. For the walker to arrive at site i after n jumps, the number of hopping to the right should be $(n+i-1)/2$, where $n+i$ must be an odd number and $1 \leqslant i \leqslant n+1$. Since the probability of hopping does not depend on site index i, we can write

$$d_{i,n} = M_{i,n}q^{(n+i-1)/2}(1-q)^{(n-i+1)/2}, \tag{C1}$$

where $M_{i,n}$ is the number of paths that do not meet the absorbing wall. Using the reflection principle of random-walk paths [34, p. 72], we get

$$M_{i,n} = \binom{n}{(n+i-1)/2} - \binom{n}{(n+i+1)/2} = \frac{n!i}{[(n+i+1)/2]![(n-i+1)/2]!}. \tag{C2}$$

Plugging Eq. (C1) with Eq. (C2) into Eq. (12), we get for $i = 2k-1$ $(n = 2m)$

$$\begin{aligned} P_{2k-1}(t) &= ie^{-t}\sum_{m=k-1}^{\infty}\frac{q^{m+k-1}(1-q)^{m-k+1}t^{2m}}{(m+k)!(m-k+1)!} \\ &= \frac{iw^i}{qt}e^{-t}\sum_{m=0}^{\infty}\frac{(x/2)^{2m+2k-1}}{(m+2k-1)!m!} \\ &= \frac{iw^i}{qt}e^{-t}I_i(x), \end{aligned} \tag{C3}$$

and for $i = 2k$ $(n = 2m+1)$

$$\begin{aligned} P_{2k}(t) &= ie^{-t}\sum_{m=k-1}^{\infty}\frac{q^{m+k}(1-q)^{m-k+1}t^{2m+1}}{(m+k+1)!(m-k+1)!} \\ &= \frac{iw^i}{qt}e^{-t}\sum_{m=0}^{\infty}\frac{(x/2)^{2m+2k}}{(m+2k)!m!} \\ &= \frac{iw^i}{qt}e^{-t}I_i(x), \end{aligned} \tag{C4}$$

where $w = \sqrt{q/(1-q)}$ and $x = 2t\sqrt{q(1-q)}$. Thus,

$$P_i(t) = \left(\sqrt{\frac{q}{1-q}}\right)^{i-1}\frac{2i}{x}I_i(x)e^{-t} \tag{C5}$$

is valid for all $i \geqslant 1$. Putting $q = (1+\varepsilon)/2$, we get Eq. (49).

[1] M. Bramson and D. Griffeath, Clustering and dispersion rates for some interacting particle-systems on Z^1, Ann. Prob. **8**, 183 (1980).

[2] D. Toussaint and F. Wilczek, Particle-antiparticle annihilation in diffusive motion, J. Phys. Chem. **78**, 2642 (1983).

[3] D. C. Torney and H. M. McConnell, Diffusion-limited reactions in one dimension, J. Phys. Chem. **87**, 1941 (1983).

[4] K. Kang and S. Redner, Scaling Approach for the Kinetics of Recombination Processes, Phys. Rev. Lett. **52**, 955 (1984).

[5] K. Kang and S. Redner, Fluctuation effects in Smoluchowski reaction-kinetics, Phys. Rev. A **30**, 2833 (1984).

[6] K. Kang and S. Redner, Fluctuation-dominated kinetics in diffusion-controlled reactions, Phys. Rev. A **32**, 435 (1985).

[7] A. A. Lushnikov, Binary reaction $1 + 1 \to 0$ in one dimension, Zh. Eksp. Teor. Fiz. **91**, 1376 (1986) [Sov. Phys. JETP **64**, 811 (1986)].

[8] L. Peliti, Renormalisation of fluctuation effects in the $A + A \to A$ reaction, J. Phys. A: Math. Gen. **19**, L365 (1986).

[9] A. A. Lushnikov, Binary reaction $1 + 1 \to 0$ in one dimension, Phys. Lett. A **120**, 135 (1987).

[10] C. R. Doering and D. ben-Avraham, Interparticle distribution functions and rate equations for diffusion-limited reactions, Phys. Rev. A **38**, 3035 (1988).

[11] J. L. Spouge, Exact Solutions for a Diffusion-Reaction Process in One Dimension, Phys. Rev. Lett. **60**, 871 (1988).

[12] B. P. Lee, Renormalization group calculation for the reaction $kA \to \emptyset$, J. Phys. A: Math. Gen. **27**, 2633 (1994).

[13] M. Henkel, E. Orlandini, and G. M. Schütz, Equivalences between stochastic systems, J. Phys. A: Math. Gen. **28**, 6335 (1995).

[14] M. Henkel, E. Orlandini, and J. Santos, Reaction-diffusion processes from equivalent integrable quantum chains, Ann. Phys. **259**, 163 (1997).

[15] P.-A. Bares and M. Mobilia, Solution of Classical Stochastic One-Dimensional Many-Body Systems, Phys. Rev. Lett. **83**, 5214 (1999).

[16] S.-C. Park, J.-M. Park, and D. Kim, Two-point correlation functions of the diffusion-limited annihilation in one dimension, Phys. Rev. E **63**, 057102 (2001).

[17] S.-C. Park and J.-M. Park, Generating function, path integral representation, and equivalence for stochastic exclusive particle systems, Phys. Rev. E **71**, 026113 (2005).

[18] D. ben Avraham and É. Brunet, On the relation between one-species diffusion-limited coalescence and annihilation in one dimension, J. Phys. A: Math. Gen. **38**, 3247 (2005).

[19] M. Doi, Second quantization representation for classical many-particle system, J. Phys. A **9**, 1465 (1976).

[20] M. Doi, Stochastic theory of diffusion-controlled reaction, J. Phys. A **9**, 1479 (1976).

[21] L. Peliti, Path integral approach to birth-death processes on a lattice, J. Phys. (France) **46**, 1469 (1985).

[22] S.-C. Park and H. Park, Driven Pair Contact Process with Diffusion, Phys. Rev. Lett. **94**, 065701 (2005).

[23] G. M. Schütz, Diffusion-limited annihilation in inhomogeneous environments, Z. Phys. B **104**, 583 (1997).

[24] G. M. Schütz and K. Mussawisade, Annihilating random walks in one-dimensional disordered media, Phys. Rev. E **57**, 2563 (1998).

[25] J.-M. Park and M. W. Deem, Disorder-induced anomalous kinetics in the $A + A \to 0$ reaction, Phys. Rev. E **57**, 3618 (1998).

[26] W. J. Chung and M. W. Deem, Numerical observation of disorder-induced anomalous kinetics in the $A + A \to \emptyset$ reaction, Physica A **265**, 486 (1999).

[27] P. Le Doussal and C. Monthus, Reaction diffusion models in one dimension with disorder, Phys. Rev. E **60**, 1212 (1999).

[28] M. J. E. Richardson and J. Cardy, The reaction process $A + A \to O$ in Sinai disorder, J. Phys. A: Math. Gen. **32**, 4035 (1999).

[29] M. Hnatich and J. Honkonen, Velocity-fluctuation-induced anomalous kinetics of the $A + A \to \emptyset$ reaction, Phys. Rev. E **61**, 3904 (2000).

[30] P. Sen and P. Ray, $A + A \to \emptyset$ model with a bias towards nearest neighbor, Phys. Rev. E **92**, 012109 (2015).

[31] S. Biswas and P. Sen, Model of binary opinion dynamics: Coarsening and effect of disorder, Phys. Rev. E **80**, 027101 (2009).

[32] S. Biswas, P. Sen, and P. Ray, Opinion dynamics model with domain size dependent dynamics: Novel features and new universality class, J. Phys.: Conf. Ser. **297**, 012003 (2011).

[33] S.-C. Park, Branching annihilating random walks with long-range attraction in one dimension, Phys. Rev. E **101**, 052125 (2020).

[34] W. Feller, *An Introduction to Probability Theory and Its Applications*, 3rd ed. (John Wiley & Sons, New York, 1968), Vol. I.

[35] J. De Coninck, F. Dunlop, and T. Huillet, Random walk weakly attracted to a wall, J. Stat. Phys. **133**, 271 (2008).

[36] M. Kim, S.-C. Park, and J. D. Noh, Coarsening dynamics of nonequilibrium chiral Ising models, Phys. Rev. E **87**, 012129 (2013).

[37] M. Kim, S.-C. Park, and J. D. Noh, Block renormalization study on the nonequilibrium chiral Ising model, Phys. Rev. E **91**, 012132 (2015).

[38] B. Daga and P. Ray, Universality classes of absorbing phase transitions in generic branching-annihilating particle systems with nearest-neighbor bias, Phys. Rev. E **99**, 032104 (2019).

[39] S.-C. Park, Crossover behaviors in branching annihilating attracting walk, Phys. Rev. E **101**, 052103 (2020).

[40] N. G. de Bruijn, *Asymptotic Methods in Analysis* (North-Holland, Amsterdam, 1970).